

## Application of mathematical empirical models to dynamic removal of lead on natural zeolite clinoptilolite in a fixed bed column

Marina Trgo\*, Nediljka Vukojević Medvidović & Jelena Perić  
Faculty of Chemistry and Technology, University of Split, Teslina 10/V, 21000 Split, Croatia

*Received 25 May 2010; accepted 19 January 2011*

This study examined the applicability of the mathematical empirical models by Bohart-Adams, Wolborska, Thomas and Yoon-Nelson on lead removal from aqueous solutions on a fixed bed of natural zeolite. Applicability of these models has been evaluated by fitting the experimental breakthrough curves with the curves obtained from the applied model. Experimental results have shown that the values of removal capacities calculated from model are close to the value of the experimentally obtained capacity at the exhaustion point. The Thomas and Yoon-Nelson models have shown excellent fit for all examined range of the breakthrough curves; therefore these models have been used for simulation of breakthrough curves for different bed depths and flow rates. The results show that the successful prediction is achieved when the empty bed contact time (EBCT) was in the experimentally confirmable range. Among all examined models, the Thomas model was found to be the most suitable one for simulation of the breakthrough curve of lead uptake on fixed bed of natural zeolite in a wide range of EBCT values.

**Keywords:** Zeolite clinoptilolite, Bohart-Adams model, Wolborska model, Thomas model, Yoon-Nelson model

The intensive development of industry is accompanied by a decrease of environmental quality. Although this development involves implementation of environmentally accepted processes, enormous quantities of industrial wastewaters are discharged into natural recipients. Industrial wastewaters are mostly loaded with heavy metals that are not biodegradable and tend to accumulate in aquatic organisms. In order to decrease the content of heavy metals in the environment, it is necessary to treat wastewaters before their discharge. The most commonly used treatments are oxidation/reduction and neutralization followed by chemical precipitation. These treatments do not usually ensure removal up to allowed concentrations. For complete removal, the suitable processes are those of tertiary treatment, such as adsorption, ion exchange, membrane techniques. The use of natural zeolites as adsorbents and ion exchangers becomes an important alternative method for removal of heavy metals from wastewaters. Ecological application of natural zeolites has been increasing in the last two decades, due to their easy exploitation, and low costs of their practical application. Their well-known chemical and thermal stability in the environment extends the scientific research to practical applications<sup>1,2</sup>.

Zeolites are hydrated aluminosilicate mineral with a cage-like structure that formed open channels of 8-10 member rings. Due to isomorphous substitution of silicon with aluminium ion, the negative structural charge is occurred, and is balanced by presence of sodium, calcium, potassium and magnesium ions in these channels. Zeolites are characterized by an outstanding capability of exchange of these alkaline and earth-alkaline cations from their structure by heavy metal cations from aqueous solution<sup>3-6</sup>. Uptake of heavy metal ions from aqueous solutions on natural zeolite is a complex process, which includes ion exchange and adsorption on the inner and outer particle surface. It is enabled by the porous zeolite structure, mineralogical heterogeneity, broken bonds and various surface imperfections on the zeolite particle<sup>7</sup>.

Column performance provides multiple repetitions of service and regeneration cycles, which makes it possible to reuse the same zeolite sample many times, and treatment of a large volume of wastewater. During the regeneration cycle, a significantly smaller volume of the concentrated metal ions solution is eluted compared to the service cycle. The regeneration effluent contains a high metal ions concentration suitable for chemical precipitation<sup>8,9</sup>.

Many researchers are trying to describe the experimental breakthrough curves using mathematical model. Most of developed models require a

\*Corresponding author (E-mail: mtrgo@ktf-split.hr)

preliminary determination of the isotherm and mass-transfer parameters, which requires additional experimentation and a non linear curve-fitting. The mathematical complexity and/or the need to know many parameters from different experiments make these models rather inconvenient for practical use. Moreover, the analytical solutions of differential equation-based models for the proposed rate mechanism are not available<sup>9-11</sup>. For that reason, various mathematical empirical models have been developed to predict the dynamic behaviour of the column<sup>11-27</sup>. This study has applied empirical models by Bohart-Adams, Wolborska, Thomas and Yoon-Nelson for describing of lead removal from aqueous solutions on a fixed bed of natural zeolite.

## Theoretical Background

### Bohart-Adams model

Bohart and Adams proposed an equation for design of the carbon adsorption column. The model assumes that the adsorption rate is proportional to both the residual capacity of the activated carbon and the concentration of the sorbing species, mainly determined by surface adsorption on the adsorbent surface sites, and is used for description of the initial part of the breakthrough curve<sup>2,13-17</sup>:

$$\ln\left(\frac{c_0}{c} - 1\right) = \ln\left(e^{\frac{k_{BA} \cdot q_{BA} \cdot H}{v}} - 1\right) - k_{BA} \cdot c_0 \cdot t \quad \dots(1)$$

where  $c_0$  is initial solute concentration (mmol/L),  $c$  is effluent solute concentration (mmol/L),  $k_{BA}$  is rate constant (L/mmol h),  $q_{BA}$  is removal capacity (mmol/L),  $H$  is bed depth (m),  $v$  is linear flow velocity (m/h) and  $t$  is service time (h).

Because the exponential term is usually much larger than unity ( $e^{\frac{k_{BA} \cdot q_{BA} \cdot H}{v}} \gg 1$ ) and with the assumption that the concentration range is considered to be low, e.g., effluent concentration  $c < 0.15 c_0$ , the Bohart Adams equation (1) can be written as:

$$\ln\left(\frac{c}{c_0}\right) = k_{BA} \cdot c_0 \cdot t - \frac{k_{BA} \cdot q_{BA} \cdot H}{v} \quad \dots(2)$$

Value of removal capacity  $q$  in mmol/g is calculated as follows<sup>17</sup>:

$$q = \frac{q_{BA} \cdot BV_S}{m} = \frac{q_{BA}}{\rho} \quad \dots(3)$$

Where  $q$  is removal capacity (mmol/g),  $BV_S$  is fixed bed volume(L),  $m$  is mass of the bed (g) and  $\rho$  is apparent density of the sorbent in the fixed bed (g/L).

From Eq. (2), the values describing the characteristic operational parameters of the column ( $k_{AB}$ , and  $q$ ) can be determined from the plot of  $\ln c/c_0$  versus  $t$  at a given bed depth, initial concentration and flow rate through the column.

### Wolborska model

The next simplified adsorption model was derived by Wolborska. The model is based on the general equation of mass transfer for the diffusion mechanism for low concentration range of breakthrough curves. The mass transfer in the fixed bed adsorption is described by the following equations<sup>15-18,20-23</sup>:

$$\frac{\partial c_b}{\partial t} + v \frac{\partial c_b}{\partial H} + \frac{\partial q}{\partial t} = D_{ax} \frac{\partial^2 c_b}{\partial H^2} \quad \dots(4)$$

where  $c_b$  is solute concentration in the bulk solution (mmol/L) and  $D_{ax}$  is axial diffusion coefficient (m<sup>2</sup>/h).

The external diffusion character of the process with a constant kinetic coefficient makes it possible to derive the following form of the kinetic equation:

$$\frac{\partial q}{\partial t} = -v_m \frac{\partial q}{\partial H} = \beta_a \cdot (c_b - c_i) \quad \dots(5)$$

where  $c_i$  is solute concentration at the solid/liquid interface (mmol/L),  $v_m$  is migration rate of the solute through the fixed bed (m/h) and  $\beta_a$  is kinetic coefficient of the external mass transfer (h<sup>-1</sup>).

For the solution of the differential equation (5) the following is assumed:  $c_i \ll c_b$ ,  $v_m \ll v$ , axial diffusion is negligible  $D_{ax} \rightarrow 0$  as  $t \rightarrow 0$ ,  $c_b = c$ , and Eq. (5) becomes:

$$\ln \frac{c}{c_0} = \frac{\beta_a \cdot c_0}{q} \cdot t - \frac{\beta_a H}{v} \quad \dots(6)$$

From the linear dependence  $\ln c/c_0$  versus  $t$ , model parameters  $\beta_a$  and  $q$  can be determined. The linear dependence of the Bohart Adams equation is the same and corresponds to the same mechanism as the Wolborska equation; therefore the same plots are used in calculation of parameters for both models.

**Thomas model**

The Thomas model is one of the most general and widely used. The model is applicable in system with a constant flow rate and no axial dispersion, and its behaviour matches the Langmuir isotherm and the second-order reversible reaction kinetics. The model has the following form<sup>13,24-26</sup>:

$$\frac{c}{c_o} = \frac{1}{1 + \exp\left[\frac{k_{Th}}{Q} \cdot (q \cdot m - c_o \cdot V)\right]} \quad \dots (7)$$

where  $k_{Th}$  is rate constant (L/mmol h),  $Q$  is flow rate (L/h),  $m$  is mass of the bed (g) and  $V$  is effluent volume (L).

The linearization of Eq. (7) yields:

$$\ln\left(\frac{c_o}{c} - 1\right) = \frac{k_{Th} \cdot q \cdot m}{Q} - \frac{k_{Th} \cdot c_o \cdot V}{Q} \quad \dots (8)$$

From the linear dependence of  $\ln[(c_o/c)-1]$  versus  $V$ , the removal capacity  $q$  and rate constant  $k_{Th}$  can be determined.

**Yoon-Nelson model**

Yoon and Nelson have developed a relatively simple model for a single component system. If  $A$  is a fraction of the solute being adsorbed in bed, and  $P$  is the fraction of the solute that remains in the effluent, the rate of adsorption can be expressed as<sup>11,15-16,19, 27</sup>:

$$-\frac{dA}{dt} = k_{YN} \cdot (t - \tau) \quad \dots (9)$$

where  $k_{YN}$  is rate constant ( $h^{-1}$ ).

With the substitution  $P = 1 - A$ , and if  $A = 0.5$  at time  $\tau$ , the integration of Eq. (9) yields:

$$\ln\left(\frac{c}{c_o - c}\right) = k_{YN} \cdot (t - \tau) \quad \dots (10)$$

where  $\tau$  is time when  $c/c_o \approx 0.5$ , h.

From the linear dependence of  $\ln[c/(c_o-c)]$  versus time  $t$ , the model parameters  $k_{YN}$  and  $\tau$  can be determined for a given bed depth, flow rate and initial concentration. Equation (10) can be written as:

$$t = \tau + \frac{1}{k_{YN}} \ln\left(\frac{c}{c_o - c}\right) \quad \dots (11)$$

If the 50 % of breakthrough is completed at  $t = \tau$ , the bed will be exhausted at  $t = 2\tau$ . For a symmetrical breakthrough curve the quantity of solute adsorbed at time  $\tau$  equals half of the removal capacity, and it is calculated relative to the initial concentration and flow rate:

$$q = \frac{c_o \cdot Q \cdot \tau}{m} \quad \dots (12)$$

Table 1 shows the equations of used mathematical empirical models.

**Experimental****Sample preparation**

The natural zeolite sample containing  $\approx 80\%$  of clinoptilolite originates from the Vranjska Banja (Serbia) deposit. The sample was crushed and sieved to the two particle size fractions of 0.1-0.5 mm and

Table 1– Mathematical relations, corresponding parameters and breakthrough curves equations of used models

Model	Mathematical equation	Linear dependences	Model parameters	Breakthrough curve
Bohart-Adams	$\ln\left(\frac{c}{c_o}\right) = k_{BA} \cdot c_o \cdot t - k_{BA} \cdot q_{BA} \cdot \frac{H}{v}$	$\ln(c/c_o)$ vs. $t$	$k_{BA}, q_{BA}, q$	$\frac{c}{c_o} = \exp\left[(k_{BA} \cdot c_o \cdot t) - (k_{BA} \cdot q_{BA} \cdot H/v)\right]$
Wolborska	$\ln\frac{c}{c_o} = \frac{\beta_a \cdot c_o \cdot t}{q} - \frac{\beta_a \cdot H}{v}$	$\ln(c/c_o)$ vs. $t$	$\beta_a, q$	$\frac{c}{c_o} = \exp\left[\left(\frac{\beta_a \cdot c_o \cdot t}{q}\right) - \left(\frac{\beta_a \cdot H}{v}\right)\right]$
Thomas	$\ln\left(\frac{c_o}{c} - 1\right) = \frac{k_{Th} \cdot q \cdot m}{Q} - \frac{k_{Th} \cdot c_o \cdot V}{Q}$	$\ln[(c_o/c)-1]$ vs. $V$	$k_{Th}, q$	$\frac{c}{c_o} = \frac{1}{1 + \exp\left[\frac{k_{Th}}{Q} \cdot (q \cdot m - c_o \cdot V)\right]}$
Yoon-Nelson	$\ln\left(\frac{c}{c_o - c}\right) = k_{YN} \cdot (t - \tau)$	$\ln[c/(c_o-c)]$ vs. $t$	$k_{YN}, \tau, q$	$\frac{c}{c_o} = \frac{c_o \cdot \exp[k_{Th} \cdot (t - \tau)]}{1 + \exp[k_{Th} \cdot (t - \tau)] \cdot c_o}$

0.6-0.8 mm and rinsed in doubly distilled water in order to remove impurities. After drying at 60°C, the samples were stored in the exsiccator. The results of XRD and chemical analysis of natural zeolite are reported elsewhere<sup>8</sup>.

#### Column study

The experiments were performed using two glass columns with the inner diameter of 12 mm and a height of 500 mm filled with zeolite samples up to 115 mm, corresponding to the bed volume of 13 cm<sup>3</sup>. The examination of Pb<sup>2+</sup> removal on the zeolite was carried out with solutions of different initial concentrations ( $c_0=1.026-2.513$  mmol Pb/L) prepared by dissolving of Pb(NO<sub>3</sub>)<sub>2</sub> in doubly distilled water without setting the initial pH value. Lead concentrations were determined complexometrically in the acid medium, using a highly selective indicator methylthymolblue<sup>28</sup>.

Service cycles were performed by passing the lead solution through the fixed zeolite bed using down flow mode. The flow rates of lead solution were kept in range of 1-3 mL/min. The flow constancy was maintained using a vacuum pump. At selected time intervals the lead concentration in effluent was determined. The process was stopped when the Pb concentration in the effluent became equal to the initial concentration in the influent. After each service cycle, the regeneration was performed with the NaNO<sub>3</sub> solution. The experimental results with breakthrough and regeneration curves are presented earlier<sup>8</sup>. In this work, the experimentally obtained breakthrough curves have been tested by Bohart-Adams, Wolborska, Thomas and Yoon-Nelson models.

In order to examine the reliability of the tested mathematical models, another four service and regeneration cycles have been performed using the same experimental procedure with zeolite particle size of 0.6-0.8 mm on zeolite bed depths of 80 mm and 40 mm (which corresponding to the bed volume of 9.04 and 4.52 cm<sup>3</sup>, respectively) with the initial

concentration of 1.026 mmol Pb/L and the flow rates of 1-3 mL/min. Experimental conditions during service and regeneration cycles are given in Table 2.

#### Results and Discussion

Application of column method in practice requires simulation of the breakthrough curves for different experimental conditions. This procedure was done in this study through the following steps: (i) determination of experimental breakthrough curves for bed depth of 115 mm and different experimental conditions<sup>8</sup>, (ii) testing of experimental breakthrough curves by mathematical empirical models and calculation of model parameters, (iii) evaluation of models and verification of calculated model parameters, (iv) simulation of breakthrough curves for bed depths of 80 mm and 40 mm (v) experimental performance of the breakthrough curves at the bed depth of 80 mm and 40 mm and (vi) comparison of simulated and experimental breakthrough curves.

#### Testing of breakthrough curves by mathematical empirical models

The empirical models by Bohart-Adams, Wolborska, Thomas and Yoon-Nelson have been used for a mathematical description of the previously published experimental results for eight service cycles<sup>8</sup>. These service cycles were performed for the zeolite bed depth of 115 mm, initial concentration of 1.026-2.513 mmol Pb/L, flow rates of lead solution of 1-3 mL/min, and for zeolite particles size of 0.1-0.5 mm and 0.6-0.8 mm. Calculations were carried out by linear regression analysis. The regression coefficient  $R^2$  was calculated as indicator of fitting of experimental points with mathematical equations of models given in Table 1. Slope and intercept were used for calculation of model parameters, and they are shown in Tables 3-5.

#### Evaluation of applied models

The equations of models shown in Table 1 include the removal capacity  $q$ , which is calculated from

Table 2—Experimental conditions for service cycles and regeneration cycles

Cycle No.	Service cycle			Regeneration cycle		
	$c_0$ (Pb) mmol/L	$\gamma_0$ (Pb) mg/L	$Q$ mL/min	$Q$ BV/h	$\gamma$ (NaNO <sub>3</sub> ) g/L	$Q$ mL/min
Bed depth 80 mm 9 <sup>th</sup>	1.026	212.5	1.0	6.63	15	1.0
Bed depth 40 mm 10 <sup>th</sup>	1.026	212.5	1.0	13.27	15	1.0
11 <sup>th</sup>	1.026	212.5	2.0	26.54	15	1.0
12 <sup>th</sup>	1.026	212.5	3.0	39.82	15	1.0

Table 3—Parameters of the Bohart-Adams and Wolborska models for different experimental conditions

Experimental conditions		Parameters of the models					$R^2$
Cycle No.	$c_0(\text{Pb})$ mmol/L	$Q$ mL/min	$k_{\text{BA}}$ L/(mmol h)	$q_{\text{BA}}$ mmol/L	$q$ mmol/g	$\beta_a$ h <sup>-1</sup>	
Particle size 0.6-0.8 mm							
2 <sup>nd</sup>	1.026	1.0	0.170	436.58	0.624	74.38	0.948
3 <sup>rd</sup>	1.026	1.0	0.184	431.14	0.616	79.25	0.938
4 <sup>th</sup>	1.759	1.0	0.228	469.73	0.671	107.13	0.995
5 <sup>th</sup>	2.513	1.0	0.274	417.15	0.596	114.11	0.981
6 <sup>th</sup>	1.026	2.0	0.637	403.04	0.576	256.70	0.933
8 <sup>th</sup>	1.026	3.0	0.790	368.44	0.527	290.94	0.926
Particle size 0.1-0.5 mm							
2 <sup>nd</sup>	1.026	1.0	0.194	436.58	0.548	82.55	0.897

Table 4—Parameters of the Thomas model for different experimental conditions

Cycle No.	$c_0(\text{Pb})$ mmol/L	$Q$ mL/min	$k_{\text{Th}}$ L/(mmol h)	$q$ mmol/g	$R^2$
Particle size 0.6-0.8 mm					
2 <sup>nd</sup>	1.026	1.0	0.214	0.600	0.975
3 <sup>rd</sup>	1.026	1.0	0.279	0.565	0.944
4 <sup>th</sup>	1.759	1.0	0.465	0.646	0.997
5 <sup>th</sup>	2.513	1.0	0.466	0.574	0.981
6 <sup>th</sup>	1.026	2.0	1.071	0.556	0.966
8 <sup>th</sup>	1.026	3.0	1.196	0.507	0.970
Particle size 0.1-0.5 mm					
2 <sup>nd</sup>	1.026	1.0	0.232	0.526	0.938

Table 5—Parameters of the Yoon-Nelson model for different experimental conditions

Experimental conditions		Parameters of the model				$R^2$
Cycle No.	$c_0(\text{Pb})$ mmol/L	$Q$ mL/min	$k_{\text{YN}}$ h <sup>-1</sup>	$\tau$ h	$q$ mmol/g	
Particle size 0.6-0.8 mm						
2 <sup>nd</sup>	1.026	1.0	0.217	88.68	0.600	0.975
3 <sup>rd</sup>	1.026	1.0	0.257	86.65	0.586	0.966
4 <sup>th</sup>	1.759	1.0	0.818	55.75	0.647	0.996
5 <sup>th</sup>	2.513	1.0	1.172	34.65	0.574	0.981
6 <sup>th</sup>	1.026	2.0	1.099	41.11	0.556	0.967
8 <sup>th</sup>	1.026	3.0	1.227	24.96	0.507	0.970
Particle size 0.1-0.5 mm						
2 <sup>nd</sup>	1.026	1.0	0.238	83.62	0.527	0.938

the linear dependences of all models. Table 6 compares calculated values  $q$  with the experimental breakthrough and exhaustion capacities  $q_B$  and  $q_E$ .

The calculated values of removal capacities are very close to the experimental capacities at the exhaustion point  $q_E$ , which indicate the applicability of tested empirical models. The parameters of each model from Tables 3-5 have been inserted into equations of breakthrough curves in Table 1, and for the chosen values of time and volume, the values of  $c/c_0$  have been calculated for each kinetic equation. The calculated values of  $c/c_0$  versus  $t$  or  $V$  have been

used to plot the breakthrough curves that were then compared with the experimental ones in Figs 1 and 2.

Figure 1 shows the comparison of experimental and calculated curves for the Thomas model, while the Fig. 2 shows that comparison for the Bohart-Adams, Wolborska and Yoon-Nelson models. Both figures show the obviously very good agreement of the Thomas and Yoon-Nelson models with experimental points for all examined ranges on the x-axis. Therefore, these models have been applied in simulation of breakthrough curves for bed depths of 80 mm and 40 mm.

**Simulation of breakthrough curves by Thomas and Yoon-Nelson models**

The simulation the breakthrough curves for zeolite bed depths of  $H = 80$  and  $40$  mm is performed using empty bed contact time (EBCT) values and the Thomas and Yoon-Nelson model parameters calculated for bed depth of  $115$  mm. EBCT includes the bed depth and flow rate, and can be expressed as:

$$EBCT = \frac{H}{v} = \frac{H}{Q/A} = \frac{d^2 \cdot \pi \cdot H}{4 \cdot Q} \quad \dots (16)$$

where  $A$  is cross-sectional area of the column ( $m^2$ ) and  $d$  is column diameter ( $m$ ).

The values of EBCT have been calculated, and are given in Table 7. The EBCT for the bed depth of

Table 6—Comparison of experimentally obtained breakthrough  $q_B$  and exhaustion capacities  $q_E$  with calculated removal capacities  $q$

Cycle No.	Experiment		Bohart-Adams and Wolborska	Thomas	Yoon-Nelson
	$q_B$ mmol/g	$q_E$ mmol/g		$q$ mmol/g	
Particle size 0.6-0.8 mm					
2 <sup>nd</sup>	0.517	0.597	0.624	0.600	0.600
3 <sup>rd</sup>	0.527	0.585	0.616	0.565	0.586
4 <sup>th</sup>	0.573	0.644	0.671	0.646	0.647
5 <sup>th</sup>	0.529	0.574	0.596	0.574	0.574
6 <sup>th</sup>	0.523	0.555	0.576	0.556	0.556
8 <sup>th</sup>	0.440	0.505	0.527	0.507	0.507
Particle size 0.1-0.5 mm					
2 <sup>nd</sup>	0.448	0.528	0.548	0.527	0.527

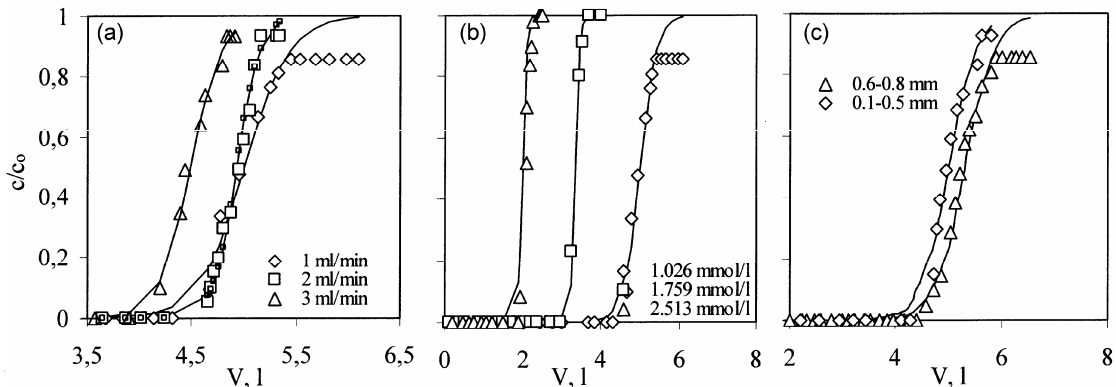


Fig. 1—Comparison of experimental (points) and breakthrough curves calculated by the Thomas model (line) for different (a) flow rates, (b) initial lead concentrations and (c) zeolite particle sizes

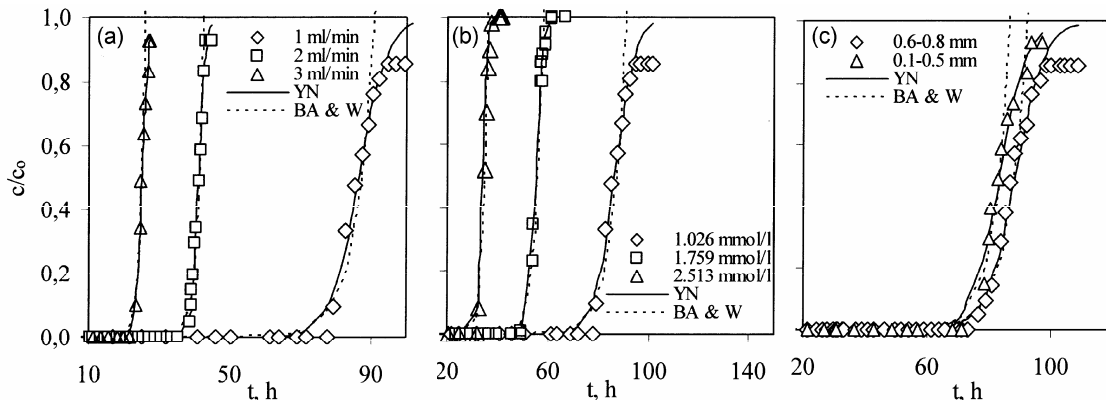


Fig. 2—Comparison of experimental (points) and breakthrough curves calculated by the Bohart-Adams and Wolborska models (dashed line) and Yoon-Nelson (full line) for different (a) flow rates, (b) initial lead concentrations and (c) zeolite particle sizes

115 mm is in range 4.33-13 min, while for bed depths of 80 mm and 40 mm is in range 1.51-9.04 min.

In order to evaluate the model parameters for the range of EBCT=1.51-9.04 min, the plots of Thomas and Yoon-Nelson model parameters ( $q$ ,  $k_{TH}$ ,  $k_{YN}$  and  $\tau$ , see Table 1) versus EBCT and flow rate are given on Fig. 3.

For the values of EBCT 9.04 min and 4.52 min, the parameters of the Thomas and Yoon-Nelson model have been evaluated from Figs 3a and 3c. For the values of EBCT 2.26 min and 1.51 min, the same

parameters have been evaluated from Figs 3b and 3d. Evaluated values are given in Table 8.

The values of evaluated parameters have been inserted into the equations of breakthrough curves in Table 1, and for the chosen values of time and volume, the  $c/c_0$  was determined for the Thomas and Yoon-Nelson models. The calculated values of  $c/c_0$  versus  $t$  or  $V$  have been used for plotting of simulated breakthrough curves for bed depths  $H = 80$  mm and 40 mm (Fig. 4.).

**Comparison of simulated and experimental breakthrough curves**

The efficiency of simulation was established by comparing the simulated curves with the curves provided in new experiments at conditions given in Table 2. Their comparison is shown in Fig. 4, where lines indicate the simulated curves and points the experimental results. Table 9 shows the

Table 7—Values of the EBCT for different flow rates at examined bed depths ( $c_0(\text{Pb})=1.026$  mmol/L)

$Q$ , mL/min	$H=115$ mm	$H=80$ mm	$H=40$ mm
	EBCT, min		
1	13.00	9.04	4.52
2	6.50	4.52	2.26
3	4.33	3.01	1.51

Table 8— Parameters of the Thomas and the Yoon-Nelson models evaluated from Fig. 3

Model	Parameter of the model	$H=80$ mm	$H=40$ mm	$H=40$ mm	$H=40$ mm
		$Q=1$ mL/min EBCT = 9.04 min	$Q=1$ mL/min EBCT = 4.52 min	$Q=2$ mL/min EBCT = 2.26 min	$Q=3$ mL/min EBCT = 1.51 min
Thomas	$k_{TH}$ , L/(mmol h)	0.75	1.19	1.07	1.19
	$q$ , mmol/g	0.550	0.556	0.580	0.574
Yoon-Nelson	$k_{YN}$ , $h^{-1}$	0.8	1.2	1.1	1.2
	$\tau$ , h	53	25	41	25

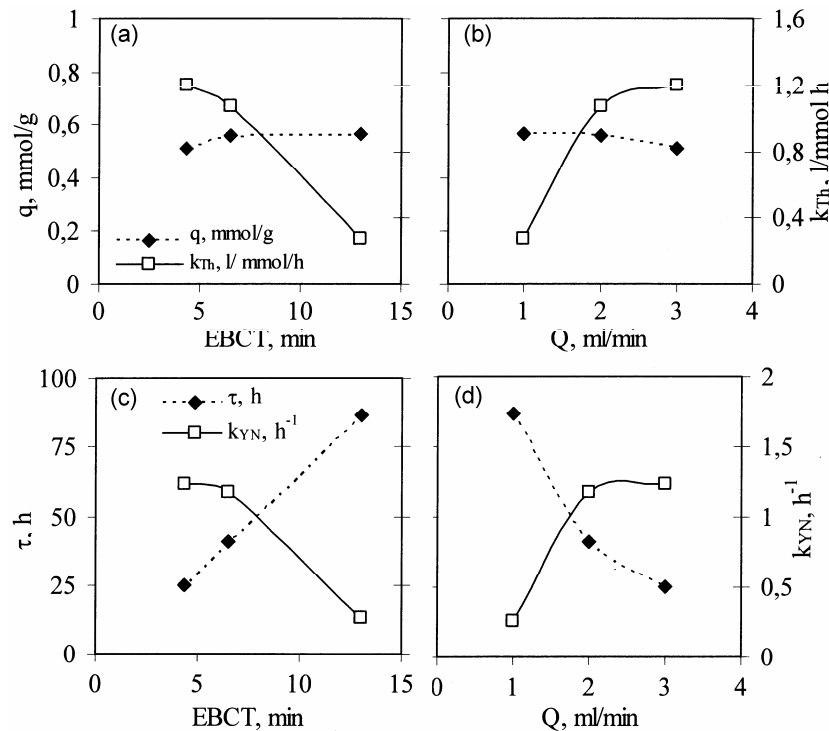


Fig. 3—Plots of model parameters versus EBCT and flow rate for (a) and (b) the Thomas model; (c) and (d) the Yoon-Nelson model

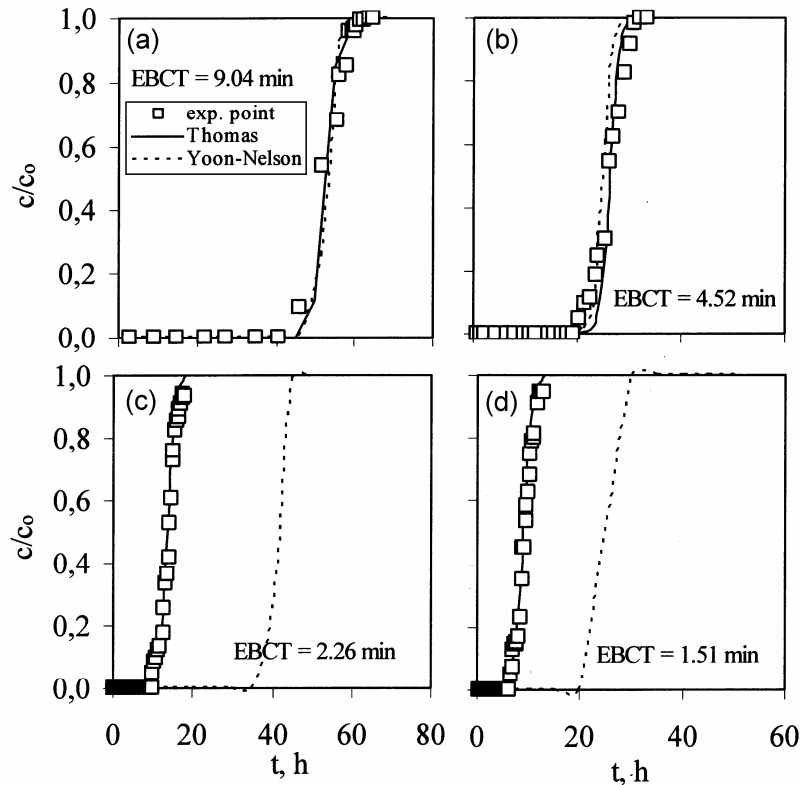


Fig. 4—Comparison of simulated and experimental breakthrough curves for different bed depths, i.e., EBCT

Table 9— Comparison of the values of breakthrough  $t_B$  and exhaustion times  $t_E$  from experimental and simulated curves

Model	Parameter of the model	$H=80$ mm	$H=40$ mm	$H=40$ mm	$H=40$ mm
		$Q=1$ mL/min EBCT = 9.04 min	$Q=1$ mL/min EBCT = 4.52 min	$Q=2$ mL/min EBCT = 2.26 min	$Q=3$ mL/min EBCT = 1.51 min
Thomas	$t_B$ , h	45.00	22.50	10.79	6.58
	$t_E$ , h	58.33	30.17	18.04	12.00
Yoon-Nelson	$t_B$ , h	49.28	22.53	38.30	22.53
	$t_E$ , h	56.68	27.45	43.68	27.45
Experiment	$t_B$ , h	43.24	20.42	10.13	6.58
	$t_E$ , h	58.50	31.83	18.03	12.10

comparison of breakthrough and exhaustion times  $t_B$  and  $t_E$  for experimental and simulated curves.

Results in Fig. 4 and data in Table 9 show a good fit of both models when EBCT = 9.04 and 4.52 min, while only the Thomas model shows a good fit for EBCT = 2.26 and 1.51 min.

The results confirm that EBCT is the characteristic parameter for prediction of the column process. The change of the bed depth and flow rate, at the constant concentration and column diameter, affects the EBCT values. Therefore the good fitting of the experimental and simulated curves is observed when the values of EBCT are in the experimentally confirmable range. This is important for scaling up of the laboratory experiment. For example, when the

column diameter increases linearly, the constant EBCT value should be maintained with the appropriate values of bed depth and flow rate.

### Conclusions

The removal of lead ions from aqueous solutions on a fixed bed of natural zeolite can be described by empirical models of Bohart-Adams, Wolborska, Thomas and Yoon-Nelson. The calculated values of removal capacities ( $q$ ) are very close to the experimental capacities at the exhaustion point ( $q_E$ ) which is determined by graphical integration of area above breakthrough curve up exhaustion point<sup>8</sup>. The Thomas and Yoon-Nelson models show excellent fitting for all examined range of breakthrough curves at bed depth of 115 mm. Therefore, the Thomas and



Yoon-Nelson model were used in simulations of breakthrough curves for bed depth 80 and 40 mm. Results show very good agreement of simulated and experimentally performed curves when the EBCT values were in the experimentally confirmable range. The performed experiments confirmed the significance of the EBCT as the main parameter for simulation procedure. Thomas model has been found to be the most suitable one for mathematical description and modelling of lead removal on a fixed bed of natural zeolite in a wide range of EBCT values.

### Acknowledgement

We are thankful to the Ministry of Science, Education and Sports of the Republic of Croatia, for financing the project (011-0000000-2239).

### References

- 1 Kurniawan T A, Chan G Y S, Lo W & Babel S, *Sci Total Environ*, 366 (2006) 409.
- 2 Wang S & Peng Y, *Chem Eng J*, 156 (2010) 11.
- 3 Stylianou M A, Hadjiconstantinou M P, Inglezakis V J, Moustakas K G & Loizidou M D, *J Hazard Mater*, 143 (2007) 575.
- 4 Perić J, Trgo M & Vukojević Medvidović N, *Water Res*, 38 (2004) 1893.
- 5 Ćurković L, Cerjan-Stefanović Š & Filipan T, *Water Res*, 31 (1997) 1379.
- 6 Petrus R & Warchol J K, *Water Res*, 39 (2005) 819.
- 7 Trgo M, Perić J & Vukojević Medvidović N, *J Hazard Mater*, B136 (2006) 938.
- 8 Vukojević Medvidović N, Perić J & Trgo M, *Sep Purif Technol*, 49 (2006) 237.
- 9 Inglezakis V J & Grigoropoulou H P, *Micropour Mesopour Mater*, 61 (2003) 273.
- 10 Warchol J K & Petrus R, *Micropour Mesopour Mater*, 93 (2006) 29.
- 11 Lin S H & Huang C Y, *J Environ Eng*, 126 (2000) 802.
- 12 Hamdaoui O, *J Hazard Mater*, 161 (2009) 737.
- 13 Aksu Z & Gonen F, *Process Biochem*, 39 (2004) 599.
- 14 Aksu Z, *Process Biochem*, 40 (2005) 997.
- 15 Hamdaoui O, *J Hazard Mater*, 138 (2006) 293.
- 16 Ghorai S & Plant K K, *Chem Eng J*, 98 (2004) 165.
- 17 Sag Y & Aktay Y, *Process Biochem*, 36 (2001) 1187.
- 18 Tran H H & Roddick F A, *Water Res*, 33 (1999) 3001.
- 19 Hutchins R A, *Chem Eng*, 20 (1973) 133.
- 20 Wolborska A & Pustelnik P, *Water Res*, 30 (1996) 2643.
- 21 Wolborska A, *Water Res*, 23 (1989) 85.
- 22 Stefanova R Y, *J Environ Sci Health*, A36 (2001) 1845.
- 23 Shen Y S, Young K & Wu M H, *Sep Sci Technol*, 38 (2003) 3513.
- 24 Hankins N P, Pliankarom S & Hilal N, *Sep Sci Technol* 39 (2004) 1347.
- 25 Yan G & Viraraghavan T, *Bioresource Technol*, 78 (2001) 243.
- 26 Juang R S, Kao H C & Chen W, *Sep Purif Technol*, 49 (2006) 36.
- 27 Yoon Y H & Nelson J H, *Am Ind Hyg Assoc J*, 45 (1984) 509.
- 28 *Complexometric Assay Methods with Triplex*, 3rd ed (E. Merck, Damstadt), p.43.